

Finding the position of tumor inhomogeneities in a gel-like model of a human breast using 3-D pulsed digital holography

Maria del Socorro Hernández-Montes

Carlos Pérez-López

Fernando Mendoza Santoyo

Centro de Investigaciones en Óptica, A.C.

Loma del Bosque 115

Col. Lomas del Campestre León

Guanajuato, México 37150

Abstract. 3-D pulsed digital holography is a noninvasive optical method used to measure the depth position of breast tumor tissue immersed in a semisolid gel model. A master gel without inhomogeneities is set to resonate at an 810 Hz frequency; then, an identically prepared gel with an inhomogeneity is interrogated with the same resonant frequency in the original setup. Comparatively, and using only an out-of-plane sensitive setup, gel surface displacement can be measured, evidencing an internal inhomogeneity. However, the depth position cannot be measured accurately, since the out-of-plane component has the contribution of in-plane surface displacements. With the information gathered, three sensitivity vectors can be obtained to separate contributions from x , y , and z vibration displacement components, individual displacement maps for the three orthogonal axes can be built, and the inhomogeneity's depth position can be accurately measured. Then, the displacement normal to the gel surface is used to find the depth profile and its cross section. Results from the optical data obtained are compared and correlated to the inhomogeneity's physically measured position. Depth position is found with an error smaller than 1%. The inhomogeneity and its position within the gel can be accurately found, making the method a promising noninvasive alternative to study mammary tumors. © 2007 Society of Photo-Optical Instrumentation Engineers. [DOI: 10.1117/1.2717515]

Keywords: pulsed digital holography; noninvasive; tumor tissue; 3-D position.

Paper 06218R received Aug. 9, 2006; revised manuscript received Nov. 27, 2006; accepted for publication Dec. 20, 2006; published online Mar. 26, 2007. This paper is a revision of a paper presented at the SPIE Conference on Seventh International Conference on Vibration 'Measurements' by Laser Techniques: Advances and Applications, Jun. 2006, Ancona, Italy. This paper presented there appears in SPIE proceedings Vol. 6345.

1 Introduction

There are several optical noninvasive methods currently used in different fields of knowledge to study object displacements and deformations. For instance, automotive and aerodynamics industries, as well as medical and biological fields use, on a daily basis, optical noninvasive methods for remote inspection, design processes, measurement of mechanical parameters (such as strain/stress), and eye correction, among many other applications. Particularly, there are two such methods that have been applied extensively and have proved their effectiveness as problem solvers: electronic speckle pattern interferometry (ESPI) and digital holography (DH). For instance, the latter has been used to measure deformations on biological tissues from a pig and on a human hand,¹ or for deformation analysis and shape measurement.² A variation of the former based on the speckle pattern contrast has been used to acquire optical tomography images for the detection of

inhomogeneities.³ Recently, DH and other techniques have been applied to measure depth position of inhomogeneities,⁴ and the detection and analysis of defects.^{5,6}

In what follows, the research done on 3-D pulsed digital holography (3-D PDH) for the detection and depth quantification of inhomogeneities within semisolid objects, also known as phantoms, is presented. The object is opaque and the inhomogeneity is placed well inside the material so that it is not visible and does not cause a dent on the object surface. Previous reported research work⁷ used an out-of-plane sensitive PDH system to detect surface microdisplacements on phantoms. The optical setup for this out-of-plane sensitivity measures the three orthogonal components of surface displacement, with the largest component being out of the plane of the object surface, e.g., the z component of a flat surface. The other two components, x , y , are there, however small, and cannot be separated from the former, i.e., the three displacement components are mixed. The inhomogeneities consisted in human breast tumors. Sinusoidal sound waves were used to scan frequencies from 20 Hz to 1 KHz to find the gel reso-

Address all correspondence to María del Socorro Hernandez, Metrología Centro de Investigaciones en Óptica, A.C. Loma del bosque 115 - León, Guanajuato 37150 Mexico; Tel: 477-441-42-00; Fax: 447-441-42-09; E-mail: mhernandez@cio.mx

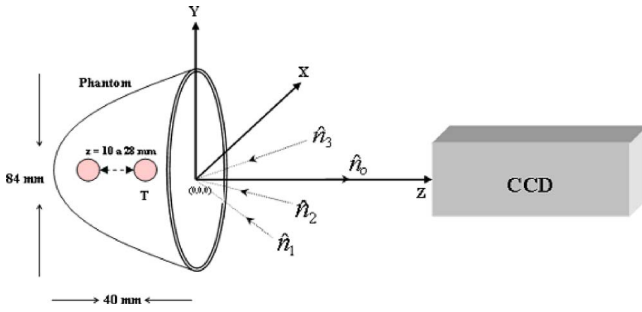


Fig. 1 The corresponding unity vectors for each of the different object illuminating source positions are shown, together with phantom dimensions and depth location of the inhomogeneities.

nant modes response. At this frequency range, two resonant modes were found, the first at 44 Hz and the second at 810 Hz. The latter frequency was chosen for the experiments, since it produced the largest surface displacement, with an input sound power of approximately 661 mW, equivalent to a pressure of 2.3×10^5 Pa. The digital hologram taken for the inhomogeneity is compared with the digital hologram taken from a phantom that does not contain an inhomogeneity. The result shows as a set of nonconcentric rings on the phantom surface. However, this is an out-of-plane sensitive system that does not render precise and reliable information regarding the actual inhomogeneity depth position, thus a 3-D PDH system was devised for its quantification.

3-D PDH employs a setup where the phantom is illuminated from three different directions.⁸ This is necessary to have from each illumination direction an equation containing the mixed surface displacement components x , y , and z , thus having three unknowns with the corresponding three equations needed to solve the problem. The usual pulsed digital hologram subtraction is performed separately: a digital hologram pair from each illumination direction. Each pair is formed with the holograms taken before (first laser pulse), e.g., at the peak of the vibration cycle, and after surface displacement (second pulse), 14 ms after the first, giving as a result a phase map directly related with the direction and magnitude of the displacement. The second pulse is fired as needed according to the mechanical wave propagating through the gel and that reaches its surface. Moving on with the process, each phase map is unwrapped to get the surface displacement data, vector \vec{d} in 3-D, via the following equation,

$$\frac{\varphi_i}{2\pi} = \frac{1}{\lambda} \vec{k}_i \cdot \vec{d}, \quad i = 1, 2, 3, \quad (1)$$

where \vec{k}_i is the unitary sensitivity vector,

$$\vec{k}_i = \hat{n}_i - \hat{n}_o, \quad i = 1, 2, 3, \quad (2)$$

with \hat{n}_i and \hat{n}_o being unitary vectors along the direction of object illumination and observation, respectively. Consider an object point P located at the origin of an orthogonal coordinate system that serves to measure in the experimental set up the location coordinates for the charge-coupled device (CCD) camera and the three sources of illumination (see Fig. 1).

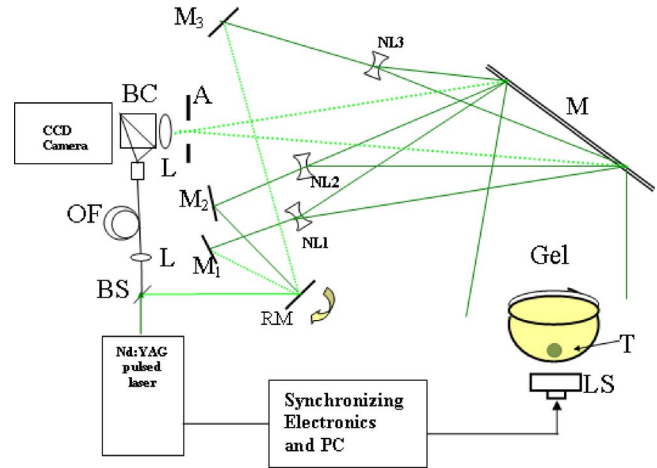


Fig. 2 The experimental setup to measure 3-D microdisplacements. RM is a rotating mirror that serves to direct the laser beam for the three illumination directions, $M_{1,2,3}$ and M are mirrors, NL are negative lenses, BS is a beamsplitter, BC is a beam combiner, LS is a loud speaker, OF is a single mode optical fiber, L is a positive lens, A is an aperture, and T is the tumor.

Each phase map for the corresponding object illumination direction is represented by $\varphi_{1,3}$, in such a way that they are combined through Eq. (1), leaving the only unknown, which is the object vector displacement \vec{d} , in all three directions x , y , and z . From these data it is now possible to individually obtain displacement information along each individual axis and thus measure the depth of the inhomogeneity within the phantom.

The characteristic unwrapped phase map for a phantom with and without an inhomogeneity is such that the concentric rings obtained for the latter are destroyed for the former, and this may be immediately noticed by simple observation of the phase map. The quantitative evaluation of such unwrapped phase maps through Eq. (1) gives the actual depth position of the inhomogeneity, a unique feature of 3-D PDH. The observed surface displacements are all in the region of micrometers.

2 Experimental Method

Three hologram pairs were obtained sequentially for five locations of the inhomogeneity: 10, 14, 16, 18 and 28 mm below the gel surface and to the outer edge of the inhomogeneity. The inhomogeneities used were tumor tissues of approximately 1 cm in diameter.

The optical arrangement is shown in Fig. 2, where a high resolution CCD is used, with 1024×1280 pixels at 12 bits. A beamsplitter divides the pulsed laser beam, Nd:YAG at 532 nm, 15-ns pulse width, and 6 m of coherence length, in two: a reference and object beam. By using a rotating mirror (RM), the latter is directed sequentially, i.e., for each hologram pair, to mirrors M_1 , M_2 , and M_3 , to illuminate the object from three different positions. The reference beam is conveyed to the CCD sensor via a single-mode optical fiber. Care was taken to match the optical path lengths by pairs to be within the laser coherence length. This arrangement is now sensitive for each object illumination direction to all x , y , and

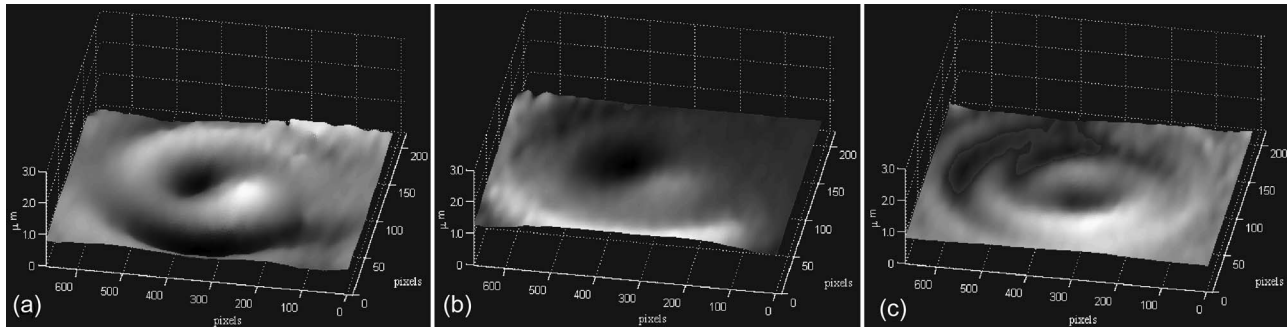


Fig. 3 (a), (b), and (c) Unwrapped phase maps for each illumination direction.

z axes. An electronic circuit was designed to synchronize and control the sinusoidal sound waves, the firing of the laser pulse, and the CCD camera trigger in such a way that the first laser pulse was fired at the peak of the sound vibration cycle, i.e., the camera shutter opens a few microseconds before this, and closes a few microseconds after the laser pulse was fired, acquiring the first digital hologram. A second laser pulse comes 14 ms after the first one, so the second digital hologram is obtained. As is commonly done in digital holography, these two holograms are subtracted after the usual Fourier algorithm routine is employed, obtaining a phase map for an illumination direction. This procedure is repeated for the other two illumination directions. Thus, three phase maps φ_{1-3} are obtained containing the direction and magnitude of the surface displacement \vec{d} in 3-D.

The phantom is a semisphere with an 8.4 cm diameter and 4 cm height, subject to sinusoidal sound waves at 810 Hz by means of an off-the-shelf speaker. The phantom center is located at the origin of the Cartesian coordinate system. The z axis data are used to evaluate the inhomogeneity depth position.

To validate and make sure that the results were repeatable, several holograms were taken for each of the phantoms at the positions given before. Since with 3-D PDH it is possible to separate individually displacement components along each axis, it is then possible to calculate normal and tangential vectors to the surface. With this in mind, it is now possible to probe that particular line that passes through the largest surface displacement. This procedure is repeated with all the available data previously taken for each object and its depth position, calibrating the 3-D PDH system in this manner.

3 Results

Several experiments were performed to verify the repeatability of the technique. Figure 3 shows three unwrapped phase maps for each illumination direction, chosen at random from many taken. It is seen that the phase pattern changes according to the illumination direction, and is clearly nonsymmetric, taken for a tumor inside the phantom. These data are used in Eq. (1) to evaluate the object surface displacement along the x , y , and z axes. Figure 4(a) shows the result in 3-D, for all three displacement components, for a 1 cm-diam tumor that gives a total phantom surface displacement of $3 \mu\text{m}$. Figure 4(b) corresponds to a phantom without any inhomogeneity and any sound present: the very small surface displacement

was due to mechanical disturbances on the optics table, a feature that shows how the surface deforms under noncontrolled arbitrary conditions. The images in this figure may be compared, and by simple observation, or by looking at the color scale at its bottom, it would be possible to decide which

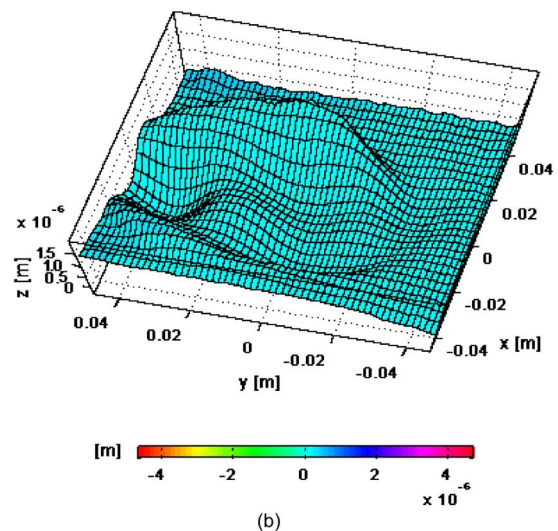
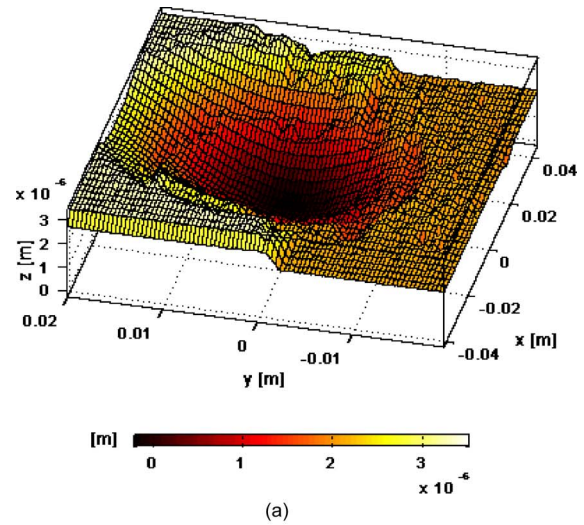


Fig. 4 From Eq. (1) and all phase maps from Fig. 3: (a) for a tumor and (b) free-standing phantom.

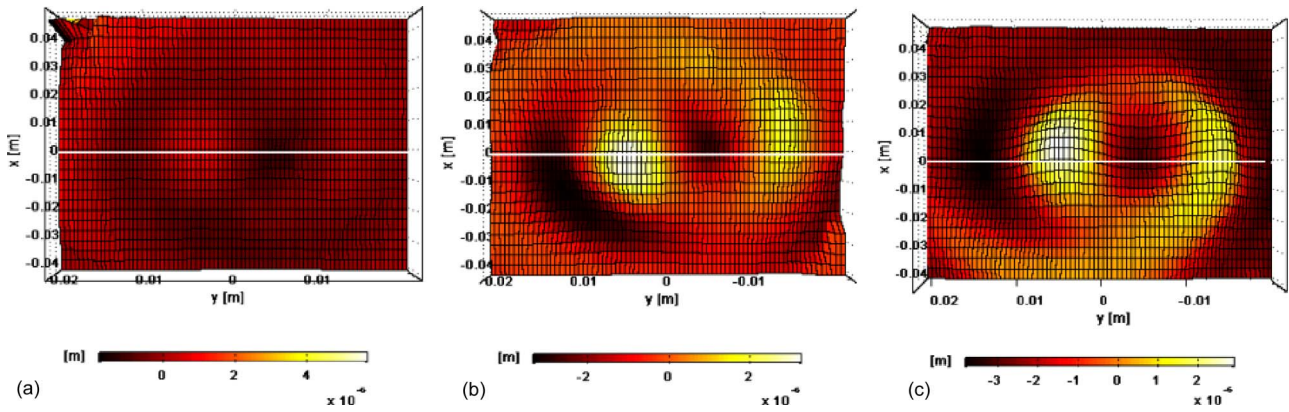


Fig. 5 Image samples chosen at random. Approximate surface displacement: (a) $-1.08 \mu\text{m}$, and (b) and (c) $-1.13 \mu\text{m}$.

sample has an inhomogeneity in it and which one does not.

Data, converted to a 78×25 pixel size, along the z axis were used to find the depth location of the inhomogeneity. Figure 5 shows images chosen at random for an inhomogeneity placed at the same depth. Several lines were scanned around the area where the inhomogeneity is located on the image, and the one corresponding to the largest surface displacement is chosen, shown in white. Vertical scans were also performed to corroborate this line data and position. The procedure was repeated for all acquired image data and for an inhomogeneity 1.2 cm diameter located 18 mm below the surface. It is pointed out here that to calibrate the system, all of the previous was done for all cited locations.

Figure 6 shows the depth location, along the z axis, of the inhomogeneity with respect to the surface. The maximum surface displacement for this tumor size and position is about $1 \mu\text{m}$. Blue, pink, and brown lines correspond to Figs. 5(a)–5(c), respectively. The actual value to determine the depth position is averaged, taking into consideration the system 0.297-mm/pixel resolution for 25 data points/line and a phantom container diameter of 84 mm . The same procedure was repeated for all images at the locations given.

Figure 7 shows the displacement results for tumor tissue with a 1-cm diameter placed at about 27 mm below the phantom surface. The maximum surface displacement, averaged, is

about $0.5 \mu\text{m}$. Figure 8 shows the error found between the optical measurements and the minimum square fit to the data, which shows a straight line that serves to predict the inhomogeneity depth location. The horizontal axis shows the real, physically measured depth of the inhomogeneity immersed in the gel, while the measurements on the vertical axis are displacement averages obtained with the optical noninvasive method dealt with here. The line scans indicate that the displacement measurements performed decrease as the depth of the inhomogeneity increases. The optical measured values are in very good agreement with the actual depth position, within an error of about 0.03% . The plot serves as a calibration chart, and thus can be used to predict from the optical data the depth of an inhomogeneity immersed in the phantom.

4 Concluding Remarks

Within the scope of this research, it is shown that 3-D pulsed digital holography is an optical noninvasive method capable of measuring with great accuracy the depth position of human tumor tissue, breast tumors, immersed in gel phantoms. Separation of the three displacement components, x , y , and z , from unwrapped phase maps quantifies their depth. The technique was tested for different inhomogeneity known positions up to depths around 28 mm below the gel surface. The results show

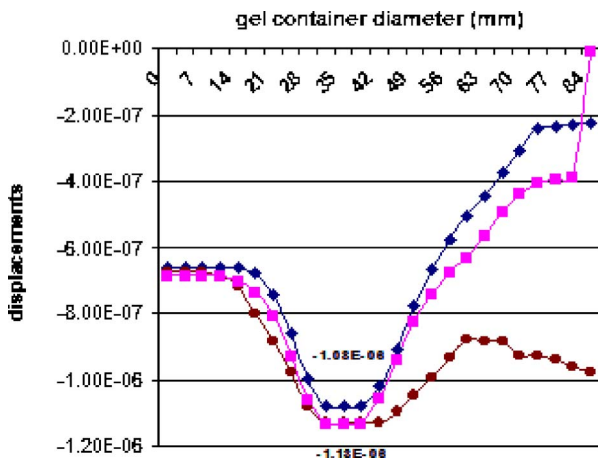


Fig. 6 Depth profile for the inhomogeneity, taken from Fig. 5.

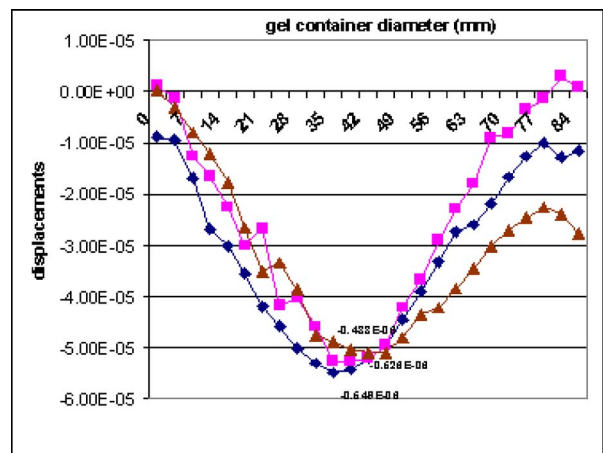


Fig. 7 Displacements for the depth profile.

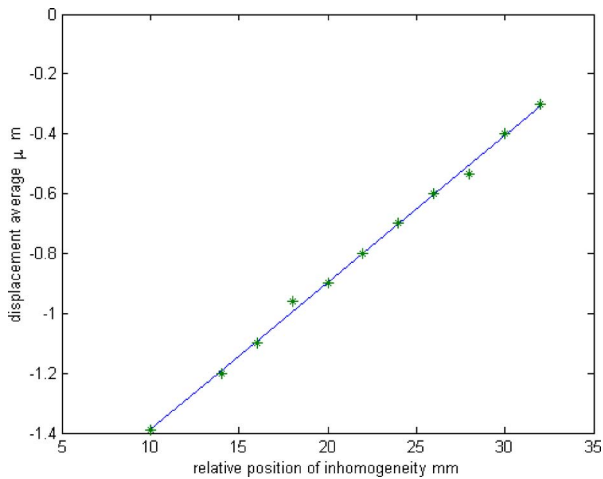


Fig. 8 Experimental results fitted to a straight line for calibration purposes.

that the optical data can be related to the depth location via a straight line fitted through the experimental results. Future research will be oriented toward the application of the method in live animals to later transfer the gained knowledge to live human tissue. The pulsed laser used delivers pulses of 15 ns width at 20 mJ of energy for the experiments conducted here. Since the illuminating object beam is expanded, the live tissue will be exposed to an average power of $0.639 \mu\text{W}/\text{cm}^2$, which is well within the limits of human tissue exposure to this type of laser. Furthermore, the sound power that may be used in live tissues will be around that used here, which is also well below the audible decibel limits. It is envisaged that

problems will arise in the placement of the human breast in the optical setup, and the finding of the optimum resonant mode frequency directly related to the type of tissue properties, like its density and fat.

Acknowledgments

The authors would like to acknowledge partial financial support from Consejo Nacional de Ciencia y Tecnología, grants 42971 and 48177.

References

1. S. Schedin, G. Pedrini, and H. J. Tiziani, "Pulsed digital holography for deformation measurements on biological tissue," *Appl. Opt.* **39**(16), 2853–2857 (2000).
2. G. Pedrini, H. J. Tiziani, and M. E. Gusev, "Pulsed digital holographic interferometry with 694- and 347 nm wavelengths," *Appl. Opt.* **39**(2), 246–249 (2000).
3. J. Li, G. Ku, and L. V. Wang, "Ultrasound-modulated optical tomography of biological tissue by use of contrast of laser speckles," *Appl. Opt.* **41**(28), 6030–6035 (2002).
4. B. C. Forget, F. Ramaz, M. Atlan, J. Selb, and A. C. Boccara, "High-contrast fast Fourier transform acousto-optical tomography of phantom tissues with a frequency-chirp modulation of the ultrasound," *Appl. Opt.* **42**(7), 1379–1383 (2003).
5. S. Schedin, G. Pedrini, H. J. Tiziani, A. K. Aggarwal, and M. E. Gusev, "Highly sensitive pulsed digital holography for built-in defect analysis with a laser excitation," *Appl. Opt.* **40**(1), 100–103 (2001).
6. M. Bashkansky, M. D. Duncan, M. Kahn, D. Lewis III, and J. Reintjes, "Subsurface defect detection in ceramics by high-speed high-resolution optical coherent tomography," *Opt. Lett.* **22**(1), 61–63 (1997).
7. M. del Socorro Hernández-Montes, C. Pérez-López, and F. Mendoza Santoyo, "Detection of biological tissue in gels using pulsed digital holography," *Opt. Express* **12**, 853–858 (2004).
8. G. Pedrini, F. Mendoza Santoyo, S. Schedin, P. Fröning, and H. J. Tiziani, "Whole 3D-digital holographic measurements of vibrating objects," *Proc. SPIE* **3823**, 53–63 (1999).